Journal of Visualized Experiments

3D printed porous cellulose nanocomposite hydrogel scaffolds

--Manuscript Draft--

Article Type:	Invited Methods Article - JoVE Produced Video
Manuscript Number:	JoVE59401R2
Full Title:	3D printed porous cellulose nanocomposite hydrogel scaffolds
Keywords:	3D printing, cellulose nanocrystals, hydrogel, porous scaffolds, biomedical applications, compression modulus
Corresponding Author:	Aji Mathew Stockholms Universitet Stockholm, Stockholm SWEDEN
Corresponding Author's Institution:	Stockholms Universitet
Corresponding Author E-Mail:	aji.mathew@mmk.su.se
Order of Authors:	Sahar Sultan
	Aji Mathew
Additional Information:	
Question	**Response**
Please indicate whether this article will be Standard Access or Open Access.	Standard Access (US$2,400)
Please indicate the **city, state/province, and country** where this article will be **filmed**. Please do not use abbreviations.	Stockholm, Sweden

Stockholm University

2019-01-08

Bing Wu, Ph.D.
Review Editor, JoVE

Sub: Submission of revised manuscript entitled **"**3D printed porous cellulose nanocomposite hydrogel scaffolds''
Ref: JoVE59401.R1

Dear Dr. Wu,

I am hereby submitting the revised version the manuscript referred above for publication in **JoVE.**

We have addressed the comments from the editor and the reviewers to the best of our ability and also provided a point by point response to the comments and suggestions. All changes are marked in blue fonts in the manuscript for easy tracking. A new author license agreement is also attached.

We are look forward for the feed back on the manuscript

I sincerely,

Professor Aji Mathew

Department of Materials and Environmental Chemistry

MMK Stockholm University
SE-106 91 Stockholm

Visiting address:
Arrhenius Laboratory
Svante Arrhenius väg 16C

Phone: +46-(0)8-161256
Mobile: +46-(0)-721474367
E-mail: aji.mathew@mmk.su.se

TITLE

3D Printed Porous Cellulose Nanocomposite Hydrogel Scaffolds

AUTHORS AND AFFILIATIONS

Sahar Sultan[1], Aji P. Mathew[1]

[1]Department of Materials and Environmental Chemistry, Stockholm University, Sweden

Corresponding Author:

Aji P. Mathew

aji.mathew@mmk.su.se

Email Addresses of Co-author:

Sahar Sultan (sahar.sultan@mmk.su.se)

KEYWORDS

3D printing, cellulose nanocrystals, hydrogel, porous scaffolds, biomedical applications, compression modulus

SUMMARY

The three critical steps of this protocol are i) developing the right composition and consistency of the cellulose hydrogel ink, ii) 3D printing of scaffolds into various pore structures with good shape fidelity and dimensions and iii) demonstration of the mechanical properties in simulated body conditions for cartilage regeneration.

ABSTRACT

This work demonstrates the use of three-dimensional (3D) printing to produce porous cubic scaffolds using cellulose nanocomposite hydrogel ink, with controlled pore structure and mechanical properties. Cellulose nanocrystals (CNCs, 69.62 wt%) based hydrogel ink with matrix (sodium alginate and gelatin) was developed and 3D printed into scaffolds with uniform and gradient pore structure (110-1100 μm). The scaffolds showed compression modulus in the range of 0.20-0.45 MPa when tested in simulated in vivo conditions (in distilled water at 37 °C). The pore sizes and the compression modulus of the 3D scaffolds matched with the requirements needed for cartilage regeneration applications. This work demonstrates that the consistency of the ink can be controlled by the concentration of the precursors and porosity can be controlled by the 3D printing process and both of these factors in return defines the mechanical properties of the 3D printed porous hydrogel scaffold. This process method can therefore be used to fabricate structurally and compositionally customized scaffolds according to the specific needs of patients.

INTRODUCTION

Cellulose is a polysaccharide consisting of linear chains of β (1-4) linked D-glucose units. It is the most abundant natural polymer on Earth and is extracted from a variety of sources, including marine animals (e.g., tunicates), plants (e.g., wood, cotton, wheat straw), and bacterial sources, such as algae (e.g., Valonia), fungi, and even amoeba (protozoa)[1,2]. Cellulose nanofibers (CNF)

and cellulose nanocrystals (CNC) with at least one dimension on nanoscale are obtained through mechanical treatments and acid hydrolysis from cellulose. They not only possess the properties of cellulose, such as potential for chemical modification, low toxicity, biocompatibility, biodegradable and renewable, but it also has nanoscale characteristics like high specific surface area, high mechanical properties, rheological and optical properties. These attractive properties have made CNFs and CNCs suitable for biomedical applications, mainly in the form of 3-dimensional (3D) hydrogel scaffolds[3]. These scaffolds require customized dimensions with controlled pore structure and interconnected porosity. Our group and others have reported 3D porous cellulose nanocomposites prepared through casting, electrospinning and freeze-drying[4-8]. However, control on the pore structure and fabrication of complex geometry is not achieved through these traditional techniques.

3D printing is an additive manufacturing technique, in which 3D objects are created layer by layer through the computer-controlled deposition of the ink[9]. The advantages of 3D printing over traditional techniques includes design freedom, controlled macro and micro dimensions, fabrication of complex architectures, customization and reproducibility. In addition, 3D printing of CNFs and CNCs also offers shear-induced alignments of nanoparticles, preferred directionality, gradient porosity and can easily be extended to 3D bioprinting[10-15]. Recently, the dynamics of CNCs alignment during 3D printing has been reported[16,17]. Advances in the field of bioprinting have enable 3D printed tissues and organs despite the involved challenge such as choice and concentration of living cells and growth factors, composition of the carrier ink, printing pressures and nozzle diameters[18-20].

The porosity and compressive strength of cartilage regenerative scaffolds are important properties that dictates its efficiency and performance. Pore size plays an important role for the adhesion, differentiation, and proliferation of cells as well as for the exchange of nutrients and metabolic waste[21]. However, there is no definite pore size that can be considered as an ideal value, some studies showed higher bioactivity with smaller pores while others showed better cartilage regeneration with larger pores. Macropores (<500 μm) facilitate tissue mineralization, nutrient supply and waste removal while micropores (150-250 μm) facilitate cell attachment and better mechanical properties[22,23]. The implanted scaffold must have sufficient mechanical integrity from the time of handling, implantation and until the completion of its desired purpose. The aggregate compressive modulus for natural articular cartilage is reported to be in the range of 0.1-2 MPa depending on age, sex and tested location[4,24-29].

In our previous work[11], 3D printing was used to fabricate porous bioscaffolds of a double crosslinked interpenetrating polymer network (IPN) from a hydrogel ink containing reinforced CNCs in a matrix of sodium alginate and gelatin. The 3D printing pathway was optimized to achieve 3D scaffolds with uniform and gradient pore structures (80-2125 μm) where nanocrystals orient preferably in the printing direction (degree of orientation between 61-76%). Here, we present the continuation of this work and demonstrates the effect of porosity on the mechanical properties of 3D printed hydrogel scaffolds in simulated body conditions. CNCs used here, were earlier reported by us to be cytocompatible and non-toxic (i.e., cell growth after 15 days of incubation was confirmed[30]). Moreover, scaffolds prepared via freeze-drying using the

same CNCs, sodium alginate and gelatin showed high porosity, high uptake of phosphate buffer saline and cytocompatibility toward mesenchymal stem cells[5]. The goal of this work is to demonstrate the hydrogel ink processing, 3D printing of porous scaffolds and the compression testing. Schematics of the processing route is shown in **Figure 1**.

PROTOCOL

1. Preparation of precursors

1.1 Preparation of cellulose nanocrystals suspension

NOTE: Isolation of cellulose nanocrystals is done according to the procedure reported by Mathew, et al[30].

1.1.1 Dilute 17 wt% suspension of cellulose nanocrystals to 2 wt% by adding distilled water to make a total volume of 2 L. Mix thoroughly using ultra sonication and use smaller batches (250-300 mL) for efficient mixing.

1.1.2 Pass the sonified suspension through the homogenizer 10 times at a pressure of 500-600 bar. At this point, a thick transparent gel of 2 wt% cellulose nanocrystals is obtained.

1.1.3 Concentrate 2 wt% cellulose nanocrystals gel to 11 wt% through centrifugations at 24,500 x *g* for 1.5 h. Decant water out in between every 30 min.

NOTE: Experiment can be paused here.

1.2 Preparation of matrix phases

1.2.1 Prepare homogeneous solution of 6 wt% sodium alginate (SA) in distilled water at 60 °C under continuous stirring.

1.2.2 Prepare homogeneous solution of 12 wt% gelatin (Gel) in distilled water at 60 °C under continuous stirring.

NOTE: Prepare a volume of 20 mL for matrix solutions and store in refrigerator.

1.3 Preparation of crosslinkers

1.3.1 Prepare the solution of 3 wt% calcium chloride in distilled water at room temperature under continuous stirring.

1.3.2 Prepare the solution of 3 wt% glutaraldehyde in distilled water at room temperature under continuous stirring.

NOTE: Prepare a volume of 50 mL for crosslinking solutions and store in room temperature. Refer to the **Table of Materials** for vendor information. Experiment can be paused here.

2. Preparation of hydrogel ink

2.1 Prepare 40 mL of hydrogel ink in a polystyrene container by mixing 11 wt% CNC, 6 wt% SA and 12 wt% Gel to obtain a wet (wt%) composition of CNC/SA/Gel/Water: 6.87/1.50/1.50/90.12.

2.2 Heat the mixture to 40 °C and mix with a spatula until a smooth paste is obtained.

2.3 Transfer the mixture into a 60 mL syringe. Pass the mixture through a series of nozzles with different diameters into another 60 mL syringe, with the help of mechanical clamp. Repeat the process until smoothly extruded filaments of hydrogel ink are obtained. Start with nozzle with biggest diameter of 800 µm, followed by 600 µm and 400 µm.

2.4 Gently centrifuge (4000xg) the syringe filled with hydrogel ink to remove trapped air.

NOTE: Experiment can be paused here.

3. Measurement of rheological properties of hydrogel

NTE: Perform the rheological properties by using a smooth cone-on-plate geometry, CP25-2-SN7617, diameter 25 mm, 2° nominal angle and gap height 0.05 mm at 25 °C.

3.1 Turn on the rheometer, air compressor and temperature control box. Initialize the software.

3.2 Mount the measuring tool in the rheometer and set zero-gap.

3.3 Extrude approximately 1 mL of the hydrogel ink onto the rheometer platform.

3.4 Measure the viscosity as a function of shear rate. Select the shear rate range from 0.001 to 1000.

3.5 After the measurement is done, clean the rheometer platform and measuring tool. Extrude 1 mL of fresh hydrogel ink again on the rheometer platform.

3.6 Measure storage moduli (G') and loss moduli (G") as a function of shear stress at a frequency of 1 Hz. Select the shear stress range from 10^3 to 10^7.

3.7 Once the tests are completed, copy the data into text file and plot rheological curves in logarithmic scale.

4. File preparation for 3D Printing

NOTE: Cura 2.4.0 software is used for designing 3D scaffolds (20 mm^3) having three types of pores. 1- Uniform pores of 0.6 mm, 2- uniform pores of 1.0 mm and 3- gradient pores of range 0.5-1 mm.

4.1 Download stereolithography (stl) file of a solid cube from thingsinverse.com and open the file in Cura.

4.2 Click the loaded model and move it to X/Y/Z : 0/0/0 mm. Click **Scale**, uncheck box for **Uniform scaling** and set the dimensions to X/Y/Z : 20/20/20 mm. Click **Rotate** and rotate the cube by 45° in XY plane.

4.3 In the side panel, in **Nozzle & Material**, select 0.4 mm and paste the profile. Select **Discov3ry complete** as the printer.

4.4 In the side panel, select **Custom** for **Print Setup**. Under **Quality** section, enter 0.2 mm for all sub sections. Under **Shell** section, enter 0 mm for all sub sections. Under **Material** section, enter 26 °C for temperature, 1 mm Diameter and 100 % Flow. Under **Speed** section, enter 30 mm/s as **Print Speed** and 120 mm/s as **Travel Speed**. Under **Support** section, uncheck the box for **Enable Support**. Under **Build Plate Adhesion** section, select **Skirt**, enter 3 mm as **Skirt Distance** and 150 mm as **Skirt/Brim Minimum length**.

4.5 For scaffolds with uniform pore size, enter 0.6 or 1 mm **Infill Line Distance** and select **Grid Infill Pattern**.

4.6 For gradient porosity scaffolds, Merging and Grouping tool is used. Right click the loaded model, select **Multiple Models**, enter 2 and press **OK**. Scale each model as X/Y/Z : 20/20/7 mm. Place the models on top of each other. Enter **Infill Line Distance** as 0.3, 0.5 and 0.7 mm for bottom, middle and top model, respectively. Select all three models (**Ctrl + A**), right click and click **Group Models**.

4.7 Save the models on the Sure Digital (SD) card. Cura automatically save the file as gcode that is read by the printer.

5. 3D printing porous scaffolds

5.1 Insert the transfer tube into the nozzle holder and connect 400 µm nozzle to it. Level the build plate to get the correct distance between the build plate and nozzle.

5.2 Load the centrifuged syringe into the cartridge and connect it to the other side of the transfer tube.

5.3 Insert the SD card into the printer, select **Purge fast** and start purging the hydrogel ink until it starts to extrude from the nozzle. Continue purging for 2-3 min to obtain a homogeneous

flow.

5.4 From the SD card, select the saved files for uniform and gradient porosity scaffolds and start printing. Keep an eye on the extrusion rate. If needed, adjust the speed and flow rate accordingly. For smaller pore size, use faster speed combined with low flow rate (50 mm/s and 70%).

NOTE: Do not touch the 3D printed scaffolds.

6. Crosslinking of 3D printed scaffolds

6.1 After the 3D printing is complete, gently add drops of 3 wt% $CaCl_2$ to the scaffold until it becomes completely wet. Wait for 5 min.

6.2 Very carefully transfer the scaffold from the printer to a 50 mL container filled with 3 wt% $CaCl_2$. Leave it overnight.

6.3 Wash thoroughly with distilled water and transfer the scaffold to a 50 mL container filled with 3 wt% glutaraldehyde. Leave it overnight.

6.4 Wash thoroughly and store the 3D printed scaffold in distilled water.

7. Compression testing

NOTE: Perform compression tests with 100 N load cell in water at 37 °C.

7.1 Fill the container equipped with submersible compression base plate with 2 L of water and start the heating system to reach 37 °C.

7.2 Initialize Bluehill Universal software and set up the testing method. Select rectangular specimen geometry and choose the option to enter dimensions before testing each sample. Set the strain rate to 2 mm/min and end of result as 80% compressive strain together with 90 N force.

7.3 In the **Measurement** section, select force, displacement, compressive stress and compressive strain. Choose the option to export data as text files for future plotting.

7.4 Set the zero extension point by using the jog controls to lower crosshead plate as close as possible to base plate.

7.5 Measure and note the dimensions of the samples to be tested.

7.6 When the water temperature reaches to 37 °C, place the sample on the base plate. Secure the sample by moving the crosshead plate so that it starts to touch the sample.

7.7 Move the water bath up, so that the plates with the sample in-between them are immersed in water.

7.6 Enter sample name and dimensions. Start the test.

7.7 After the test is complete, first move the water bath down and then raise the crosshead plate.

7.8 Remove the sample and its pieces, if any, clean both the plates and load a new sample.

7.9 After all the samples are tested, export the raw data. Plot compressive stress vs. compressive strain curves and determine the compressive tangent modulus at strain values of 1-5 % and 25-30 %.

NOTE: Place the gradient cube in such a way that the larger holes face the stationery base plate. First secure the scaffold in between the grips and then start/stop the measurement.

REPRESENTATIVE RESULTS

CNCs based nanocomposite hydrogel ink shows a strong non-Newtonian shear thinning behavior (**Figure 2a**). The apparent viscosity of 1.55 × 10^5 Pa.s at a low shear rate (0.001 s^{-1}) drops by five orders of magnitude to a value of 22.60 Pa.s at a shear rate of 50 s^{-1} (≈50 s^{-1} being a typical shear rate experienced during 3D printing)[31]. The hydrogel ink exhibits a viscoelastic solid behavior, as the storage modulus G' (4.42×10^7 Pa) is an order of magnitude greater than the loss modulus G'' (8.26×10^6 Pa) at low shear stress, with a well-defined dynamic yield stress value (G'=G'') of 5.59×10^4 Pa (**Figure 2b**). The 3D printed porous nanocomposite hydrogel scaffolds are in shown in **Figure 3**. For all the printed scaffolds, the shape and dimensions are very well retained after printing as well as after double crosslinking. The pore sizes of the scaffolds, 110-1100 µm, are in the range of 100-400 µm that is considered a benchmark for cartilage regeneration[32].

The 3D printed scaffolds were tested in compression mode. This is the preferred mode of mechanical testing for cartilage materials because the role of natural cartilage is to bear loads in compression. To mimic the in vivo conditions, scaffolds were tested in water at 37 °C. **Table 1** and **Figure 4a** represents the compressive data obtained for different porous nanocomposite hydrogel scaffolds at a strain rate of 2 mm/min. At low strain rates (1-5%), the compressive modulus (~ 0.17 MPa) is more or less similar for all types of porous scaffolds. This shows that the elastic nature of the hydrogel ink is preserved even in the presences of the macropores. However, at high strain rates (25-30%), the highest modulus of 0.45 MPa is obtained for reference scaffold with no porosity. However, as soon as the pore size increases, the modulus decreases, due to the decrease in density indicating the expected relationship between porosity of the scaffolds and the corresponding mechanical properties. In case of the gradient porous scaffolds, the modulus is higher (0.34 MPa) as compared to uniform porous scaffolds (0.20 and 0.26 MPa) because of the presence of smaller pore sizes and more solid walls. Furthermore, the

compressive modulus of the 3D hydrogel scaffolds increases as the compression rate increases (**Figure 4b**), exhibiting and mimicking the viscoelasticity of natural cartilage tissues that is considered favorable for load bearing scaffolds[33]. The compressive modulus of 0.20 MPa at strain rate of 2 mm/min increases to 0.35 MPa at 5 mm/min and further increases to 0.47 MPa at 120 mm/min and is in the range reported for natural cartilage (i.e., compressive modulus of 0.1-2 MPa).

FIGURE AND TABLE LEGENDS

Figure 1. Schematics of the processing route. (**a**) Preparation of the nanocomposite hydrogel ink. (**b**) 3D printing porous scaffolds. (**c**) Double crosslinking of 3D printed scaffolds. (**d**) Compression testing of 3D porous scaffolds in water at 37 °C.

Figure 2. Log–log plots of nanocomposite hydrogel ink. (**a**) Viscosity vs. shear rate and (**b**) G' and G'' vs. shear stress.

Figure 3. 3D printed porous scaffolds. Scale: 500 µm. (**a**) Reference with no holes. (**b**) 1 mm pore size. (**c**) 0.60 mm pore size. (**d**) Gradient porosity 110-800 µm.

Figure 4. Representative stress-strain curves for 3D printed porous nanocomposite hydrogel scaffolds. (**a**) At constant strain rate of 2 mm/s. (**b**) At different strain rates for 1 mm pore size scaffold.

Table 1. Compression data for 3D printed nanocomposite hydrogel scaffolds.

DISCUSSION

3D printing requires suitable rheological properties of the hydrogel ink. The high viscosity ink will require extreme pressures for its extrusion while low viscosity ink will not maintain its shape after extrusion. The viscosity of the hydrogel ink can be controlled through the concentration of the ingredients. As compared to our previous work[11], the solid content of the hydrogel ink is increased from 5.4 to 9.9 wt% resulting in concentrated hydrogel ink which helps to improve the resolution of the printed scaffold. It may be noted that, unlike long flexible CNFs, rigid rod like CNCs can produce inks with higher solid contents at a given viscosity due to the absences of physical entanglements[14]. Another important aspect that affect printability is the homogeneity of the ink. It was noted that heating the hydrogel ink at a temperature of 40 °C promotes the homogeneous mixing of CNCs with the matrix phase. To further ensure the smoothness of the hydrogel ink, it was passed through a series of nozzles, starting with the biggest diameter of 800 µm, then 600 µm and finally 400 µm. During these passes, the nozzle can be clogged which indicates the presences of big lumps but after these passes the hydrogel ink extruded effortlessly in the form of a continuous filament. The nozzle movement to obtain 3D printed constructs is also of great importance as indicated by our previous work[11]. The nozzle pathway should avoid repetitive movements and excess depositions of the hydrogel ink so that the resolution of the 3D print is preserved.

The porosity obtained in the 3D printed hydrogel scaffolds is in the acceptable range as compared to the targeted porosity (**Table 1**). An exact match cannot be expected because of the swelling nature of the hydrogel ink. The consistency of the hydrogel ink is an important factor especially when *ex-situ* crosslinking has to be done, i.e. crosslinking after the printing of the 3D construct. It was noted that the hydrogel ink was concentrated enough (solid content of 9.9 wt%) to maintain its shape, structure and dimensions during and after the printing process.

The pore size of the scaffold plays an essential role in cell interactions, oxygen diffusion and waste removal together with its mechanical properties to perform and support the desired functionality. Scaffolds with gradient porosity have the ability to better represent the actual in vivo conditions where cells are exposed to layers of different tissues with varying structural properties[22,23,34]. The porosity and mechanical properties are inversely related but the composition of the hydrogel scaffold can play an important role. CNCs has been selected as the main ingredient of the hydrogel ink because of its well-known mechanical properties[2,35,36]. The hydrogel ink fabricated here, possess its elasticity even in the presences of the pores, has an optimal pore size (110-1100 µm) and a suitable compressive modulus (0.20-0.45 MPa) required for cartilage regeneration applications.

Compression testing was done in water and at body temperature to mimic the in vivo conditions as much as possible. There was no drying step involved between 3D printing and mechanical testing. In natural tissues, a porosity gradient is observed rather than one uniform pore size. The same is true for compression values for load bearing natural tissues, as the compressive modulus depends on the age, sex and on the tested location.

The advantage with the study presented here is that the final porosity and compressive modulus values of 3D porous scaffold can be controlled and customized through hydrogel ink composition and 3D printing process. This protocol is flexible and can be modified according to the specific requirements. The 3D printing is a powerful technique and can be explored in future to develop scaffolds with complex structural and compositional features. Multi material dispensing can introduce revolution by controlling the composition of the scaffolds, concentration of cells or growth factors, structural features such as directionality or porosity, mechanical properties and degradation rate in different parts of the 3D constructs.

ACKNOWLEDGMENTS

This study is financially supported by Knut and Alice Wallenberg Foundation (Wallenberg Wood Science Center), Swedish Research Council,VR (Bioheal, DNR 2016-05709 and DNR 2017-04254).

DISCLOSURES

The authors have nothing to disclose.

REFERENCES

1. Moon, R.J., Martini, A., Nairn, J., Simonsen, J. & Youngblood, J. Cellulose nanomaterials review: structure, properties and nanocomposites. *Chemical Society Reviews.* **40** (7), 3941-3994

(2011).

2. Dufresne, A. Nanocellulose: a new ageless bionanomaterial. *Materials Today.* **16** (6), 220-227 (2013).

3. Chinga-Carrasco, G. Potential and limitations of nanocelluloses as components in biocomposite inks for three-dimensional bioprinting and for biomedical devices. *Biomacromolecules.* **19** (3), 701-711 (2018).

4. Naseri, N., Poirier, J., Girandon, L., Fröhlich, M., Oksman, K. & Mathew, A.P. 3-Dimensional porous nanocomposite scaffolds based on cellulose nanofibers for cartilage tissue engineering: tailoring of porosity and mechanical performance. *Royal Society of Chemistry Advances.* **6** (8), 5999-6007 (2016).

5. Naseri, N., Deepa, B., Mathew, A.P., Oksman, K. & Girandon, L. Nanocellulose-Based Interpenetrating Polymer Network (IPN) Hydrogels for Cartilage Applications. *Biomacromolecules.* **17** (11), 3714-3723 (2016).

6. Naseri, N., Mathew, A.P., Girandon, L., Fröhlich, M. & Oksman, K. Porous electrospun nanocomposite mats based on chitosan–cellulose nanocrystals for wound dressing: effect of surface characteristics of nanocrystals. *Cellulose.* **22** (1), 521-534 (2015).

7. Xing, Q., Zhao, F., Chen, S., McNamara, J., DeCoster, M.A. & Lvov, Y.M. Porous biocompatible three-dimensional scaffolds of cellulose microfiber/gelatin composites for cell culture. *Acta Biomaterialia.* **6** (6), 2132-2139 (2010).

8. Nandgaonkar, A., Krause, W. & Lucia, L. Fabrication of cellulosic composite scaffolds for cartilage tissue engineering. In: *Nanocomposites for musculoskeletal tissue regeneration.* Elsevier, 187-212 (2016).

9. Gross, B.C., Erkal, J.L., Lockwood, S.Y., Chen, C. & Spence, D.M. Evaluation of 3D printing and its potential impact on biotechnology and the chemical sciences. *Analytical Chemistry.* **86** (7), 3240-3253, (2014).

10. Markstedt, K., Mantas, A., Tournier, I., Martínez Ávila, H., Hägg, D. & Gatenholm, P. 3D bioprinting human chondrocytes with nanocellulose–alginate bioink for cartilage tissue engineering applications. *Biomacromolecules.* **16** (5), 1489-1496 (2015).

11. Sultan, S. & Mathew, A.P. 3D printed scaffolds with gradient porosity based on a cellulose nanocrystal hydrogel. *Nanoscale.* **10**, 4421-4431, (2018).

12. Sultan, S., Siqueira, G., Zimmermann, T. & Mathew, A.P. 3D printing of nano-cellulosic biomaterials for medical applications. *Current Opinion in Biomedical Engineering.* **2**, 29-34, (2017).

13. Sultan, S., Abdelhamid, H.N., Zou, X. & Mathew, A.P. CelloMOF: Nanocellulose Enabled 3D Printing of Metal–Organic Frameworks. *Advanced Functional Materials.* 1805372-1805384 (2018).

14. Siqueira, G.*,* et al. Cellulose Nanocrystal Inks for 3D Printing of Textured Cellular Architectures. *Advanced Functional Materials.* **27** (12), 1604619-1604629, (2017).

15. Wang, J.*,* et al. All-in-One Cellulose Nanocrystals for 3D Printing of Nanocomposite Hydrogels. *Angewandte Chemie International Edition.* **57** (9), 2353-2356 (2018).

16. Hausmann, M.K.*,* et al. Dynamics of Cellulose Nanocrystal Alignment during 3D Printing. *ACS Nano.* **12** (7), 6926-6937 (2018).

17. Liu, Y.*,* et al. Nanoscale assembly of cellulose nanocrystals during drying and redispersion. *ACS Macro Letters.* **7** (2), 172-177 (2018).

18. Murphy, S.V. & Atala, A. 3D bioprinting of tissues and organs. *Nature Biotechnology.* **32** (8), 773-785 (2014).

19. Pati, F.*,* et al. Printing three-dimensional tissue analogues with decellularized extracellular matrix bioink. *Nature communications.* **5**, 3935 (2014).

20. Xia, Z., Jin, S. & Ye, K. Tissue and organ 3D bioprinting. *SLAS TECHNOLOGY: Translating Life Sciences Innovation.* **23** (4) 301-314 (2018).

21. Zhang, Q., Lu, H., Kawazoe, N. & Chen, G. Pore size effect of collagen scaffolds on cartilage regeneration. *Acta Biomaterialia.* **10** (5), 2005-2013 (2014).

22. Loh, Q.L. & Choong, C. Three-dimensional scaffolds for tissue engineering applications: role of porosity and pore size. *Tissue Engineering, Part B: Reviews.* **19** (6), 485-502 (2013).

23. Bružauskaitė, I., Bironaitė, D., Bagdonas, E. & Bernotienė, E. Scaffolds and cells for tissue regeneration: different scaffold pore sizes—different cell effects. *Cytotechnology.* **68** (3), 355-369 (2016).

24. Zhang, L., Hu, J. & Athanasiou, K.A. The role of tissue engineering in articular cartilage repair and regeneration. *Critical Reviews™ in Biomedical Engineering.* **37** (1-2) (2009).

25. Athanasiou, K., Rosenwasser, M., Buckwalter, J., Malinin, T. & Mow, V. Interspecies comparisons of in situ intrinsic mechanical properties of distal femoral cartilage. *Journal of Orthopaedic Research.* **9** (3), 330-340 (1991).

26. Schinagl, R.M., Gurskis, D., Chen, A.C. & Sah, R.L. Depth-dependent confined compression

485 modulus of full-thickness bovine articular cartilage. *Journal of Orthopaedic Research.* **15** (4),
486 499-506 (1997).
487
488 27. Athanasiou, K., Niederauer, G. & Schenck, R. Biomechanical topography of human ankle
489 cartilage. *Annals Biomedical Engineering.* **23** (5), 697-704 (1995).
490
491 28. Athanasiou, K.A., Liu, G.T., Lavery, L.A., Lanctot, D.R. & Schenck, R.C.,Jr. Biomechanical
492 topography of human articular cartilage in the first metatarsophalangeal joint. *Clinical*
493 *Orthopaedics and Related Research.* **348**, 269-281 (1998).
494
495 29. Guilak, F., Jones, W.R., Ting-Beall, H.P. & Lee, G.M. The deformation behavior and
496 mechanical properties of chondrocytes in articular cartilage. *Osteoarthritis and Cartilage.* **7** (1),
497 59-70 (1999).
498
499 30. Mathew, A.P., Oksman, K., Karim, Z., Liu, P., Khan, S.A. & Naseri, N. Process scale up and
500 characterization of wood cellulose nanocrystals hydrolysed using bioethanol pilot plant.
501 *Industrial Crops and Products.* **58**, 212-219 (2014).
502
503 31. Compton, B.G. & Lewis, J.A. 3D-printing of lightweight cellular composites. *Advanced*
504 *Materials.* **26** (34), 5930-5935 (2014).
505
506 32. Sarem, M., Moztarzadeh, F. & Mozafari, M. How can genipin assist gelatin/carbohydrate
507 chitosan scaffolds to act as replacements of load-bearing soft tissues? *Carbohydrate Polymers.*
508 **93** (2), 635-643 (2013).
509
510 33. Chia, H.N. & Hull, M. Compressive moduli of the human medial meniscus in the axial and
511 radial directions at equilibrium and at a physiological strain rate. *Journal of orthopaedic*
512 *research.* **26** (7), 951-956 (2008).
513
514 34. Zhang, K., Fan, Y., Dunne, N. & Li, X. Effect of microporosity on scaffolds for bone tissue
515 engineering. *Regenerative biomaterials.* **5** (2), 115-124 (2018).
516
517 35. Lin, N. & Dufresne, A. Nanocellulose in biomedicine: Current status and future prospect.
518 *European Polymer Journal.* **59**, 302-325 (2014).
519
520 36. Domingues, R.M., Gomes, M.E. & Reis, R.L. The potential of cellulose nanocrystals in tissue
521 engineering strategies. *Biomacromolecules.* **15** (7), 2327-2346 (2014).
522

Figure 1

Click here to access/download;Figure;Figure

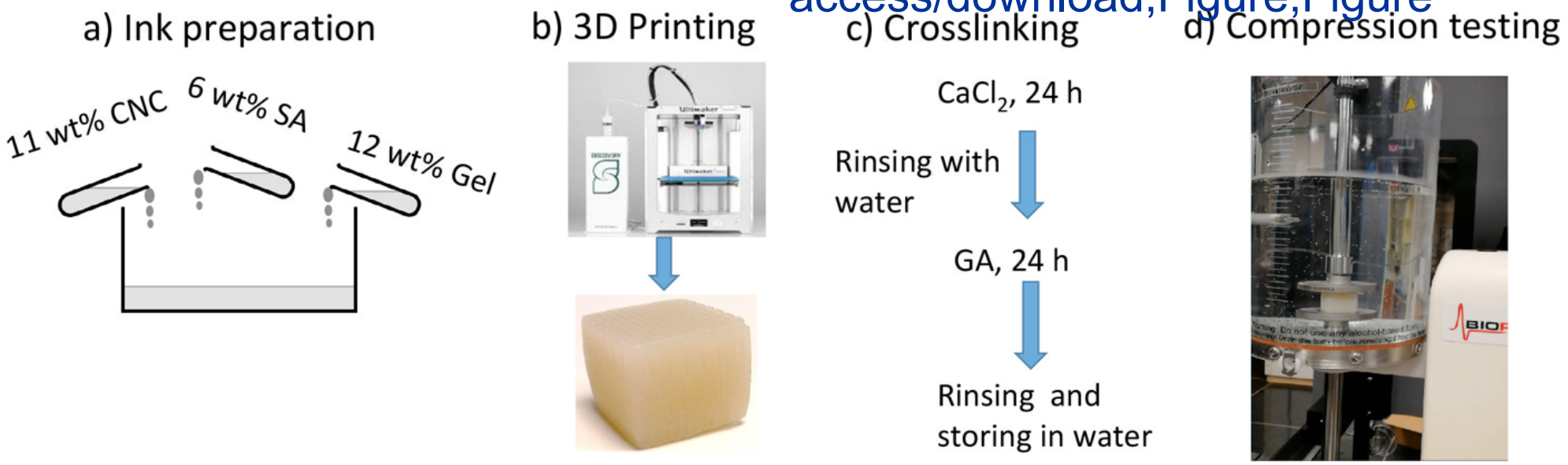

Figure 2

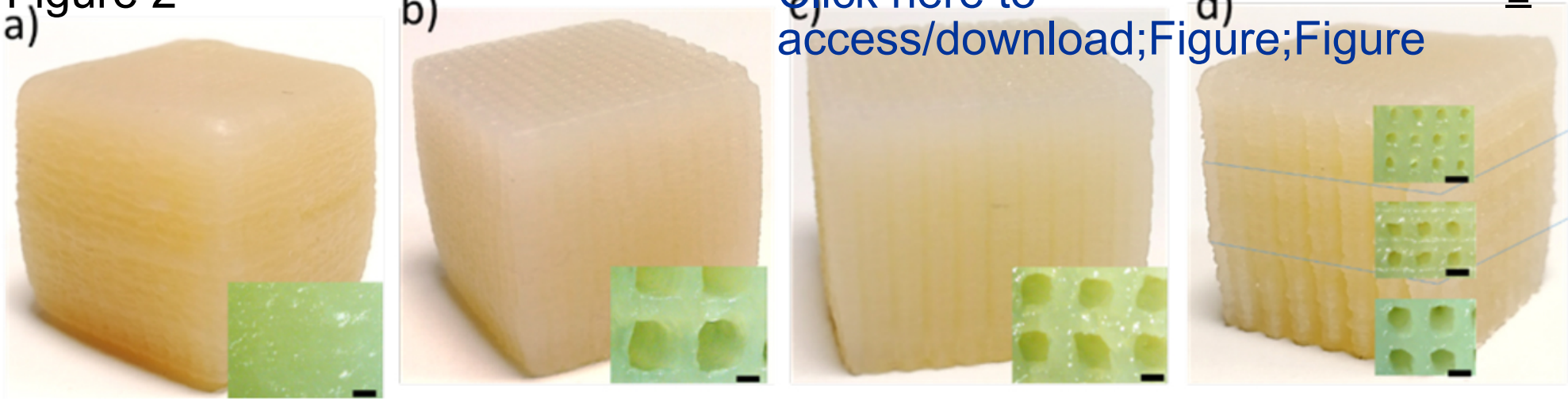

Click here to access/download;Figure;Figure

Figure 3

Click here to access/download;Figure;Figure

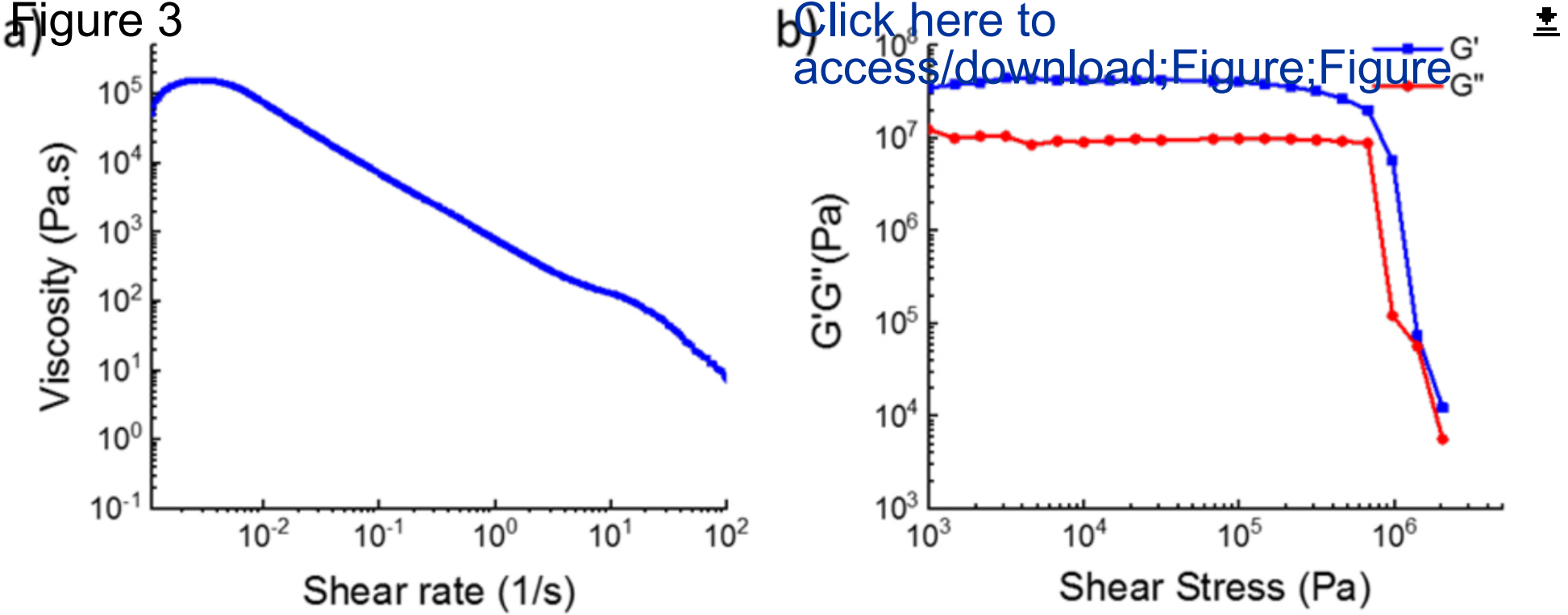

Figure 4

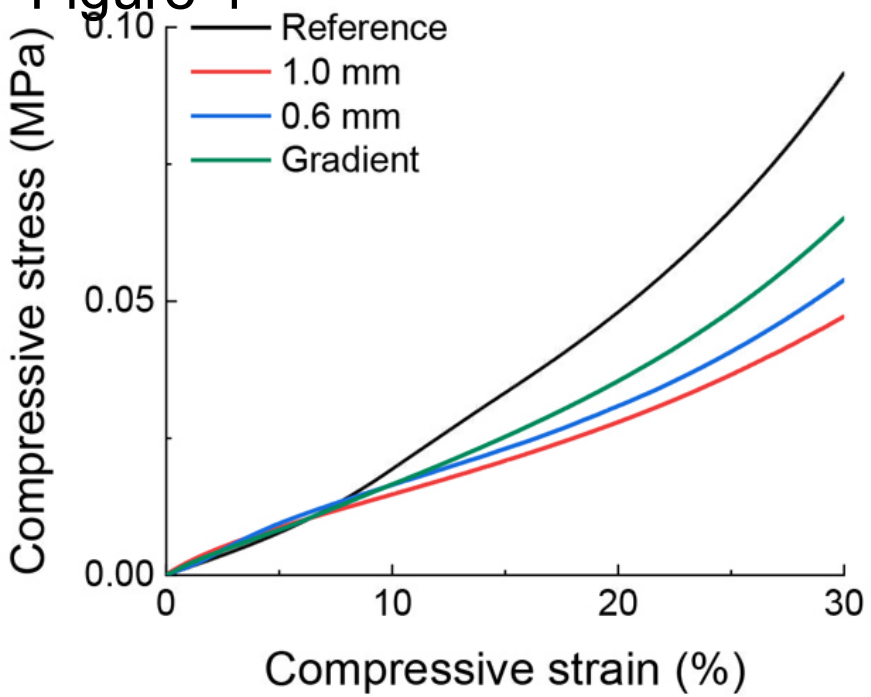

Click here to access/download;Figure;Figure

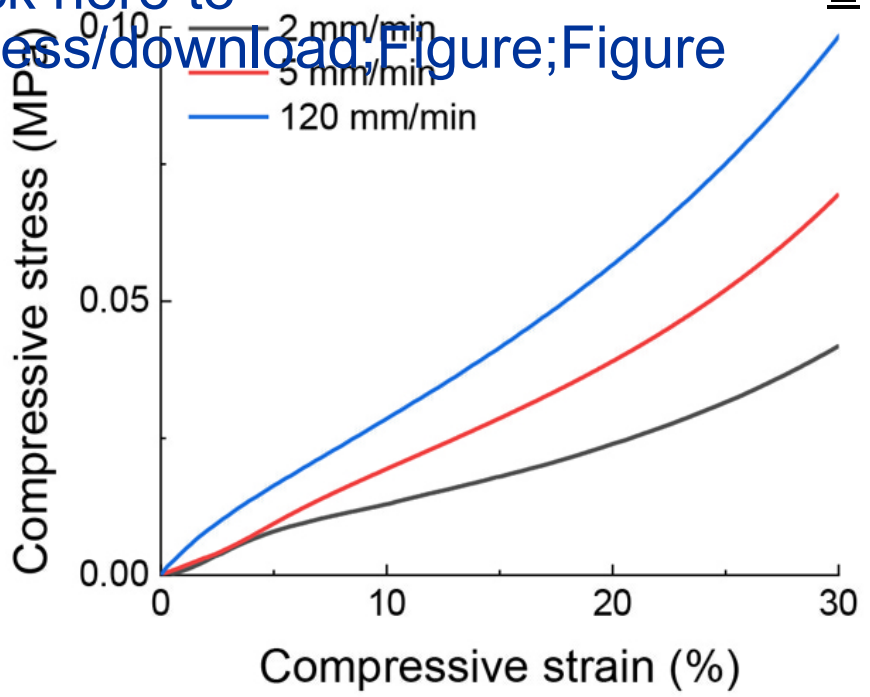

Table

Target pore size (μm)	Average pore size (μm)
Reference	0
1000	850-1100
600	480-650
Gradient	110-800

Compressive modulus at 1-5 % strain (MPa)
0.19 ± 0.04
0.17 ± 0.02
0.16 ± 0.01
0.16 ± 0.01

Compressive modulus at 25-30 % strain (MPa)
0.45 ± 0.03
0.2 ± 0.01
0.26 ± 0.05
0.34 ± 0.04

Table of Materials

Click here to access/download;Table of Materials;Table of Materials.xls

Name of Material/ Equipment	Company	Catalog Number
60 mL syringe	Structur3D Printing	
Alginic acid sodium salt	Sigma-Aldrich	9005-38-3
Anhydrous calcium chloride	Sigma-Aldrich	10043-52-4
Clamps, three pronged, Talon	VWR	241-0404
Cura 2.4.0	Ultimaker	
Discov3ry Complete	Structur3D Printing	
Gelatin from bovine skin	Sigma-Aldrich	9000-70-8
Glutaraldehyde solution 50 wt. % in H2O	Sigma-Aldrich	111-30-8
homogenizer	SPX	APV-2000
Instron 5960	Instron	
Physica MCR 301 rheometer	Anton Paar	
Sorvall Lynx 6000 centrifuge	AB Ninolab	s/n 41881692
stainless steel nozzle	Structur3D Printing	
thingsinverse	MakerBot's	
ultra sonication	Qsonica, LLC	Q500
Unbarked wood chips	Norway spruce (Picea abies)	

Comments/Description

102 mm, Dual adjustment clamp, large, clamp extension 127 mm
Free slicing software
Ultimaker 2+ 3D printer integrated with Discov3ry paste extruder

Instron 5960, Biopuls Bath, 100 N load cell, 37 °C,
CP25-2-SN7617, gap height 0.05 mm, 25 °C
F12-rotor (6x500 ml)
800, 600 and 400 µm
sharing and downloading 3D printable things in form of stl files

dry matter content of 50–55%

1 Alewife Center #200
Cambridge, MA 02140
tel. 617.945.9051
www.jove.com

ARTICLE AND VIDEO LICENSE AGREEMENT

Title of Article: 3D printed porous cellulose nanocomposite hydrogel scaffolds

Author(s): Sahar Sultan , Aji P Mathew

Item 1 (check one box): The Author elects to have the Materials be made available (as described at http://www.jove.com/author) via: [X] Standard Access [ ] Open Access

Item 2 (check one box):

[X] The Author is NOT a United States government employee.

[ ] The Author is a United States government employee and the Materials were prepared in the course of his or her duties as a United States government employee.

[ ] The Author is a United States government employee but the Materials were NOT prepared in the course of his or her duties as a United States government employee.

ARTICLE AND VIDEO LICENSE AGREEMENT

1. Defined Terms. As used in this Article and Video License Agreement, the following terms shall have the following meanings: "**Agreement**" means this Article and Video License Agreement; "**Article**" means the article specified on the last page of this Agreement, including any associated materials such as texts, figures, tables, artwork, abstracts, or summaries contained therein; "**Author**" means the author who is a signatory to this Agreement; "**Collective Work**" means a work, such as a periodical issue, anthology or encyclopedia, in which the Materials in their entirety in unmodified form, along with a number of other contributions, constituting separate and independent works in themselves, are assembled into a collective whole; "**CRC License**" means the Creative Commons Attribution-Non Commercial-No Derivs 3.0 Unported Agreement, the terms and conditions of which can be found at: http://creativecommons.org/licenses/by-nc-nd/3.0/legalcode; "**Derivative Work**" means a work based upon the Materials or upon the Materials and other pre-existing works, such as a translation, musical arrangement, dramatization, fictionalization, motion picture version, sound recording, art reproduction, abridgment, condensation, or any other form in which the Materials may be recast, transformed, or adapted; "**Institution**" means the institution, listed on the last page of this Agreement, by which the Author was employed at the time of the creation of the Materials; "**JoVE**" means MyJove Corporation, a Massachusetts corporation and the publisher of *The Journal of Visualized Experiments;* "**Materials**" means the Article and / or the Video; "**Parties**" means the Author and JoVE; "**Video**" means any video(s) made by the Author, alone or in conjunction with any other parties, or by JoVE or its affiliates or agents, individually or in collaboration with the Author or any other parties, incorporating all or any portion of the Article, and in which the Author may or may not appear.

2. Background. The Author, who is the author of the Article, in order to ensure the dissemination and protection of the Article, desires to have the JoVE publish the Article and create and transmit videos based on the Article. In furtherance of such goals, the Parties desire to memorialize in this Agreement the respective rights of each Party in and to the Article and the Video.

3. Grant of Rights in Article. In consideration of JoVE agreeing to publish the Article, the Author hereby grants to JoVE, subject to **Sections 4** and **7** below, the exclusive, royalty-free, perpetual (for the full term of copyright in the Article, including any extensions thereto) license (a) to publish, reproduce, distribute, display and store the Article in all forms, formats and media whether now known or hereafter developed (including without limitation in print, digital and electronic form) throughout the world, (b) to translate the Article into other languages, create adaptations, summaries or extracts of the Article or other Derivative Works (including, without limitation, the Video) or Collective Works based on all or any portion of the Article and exercise all of the rights set forth in (a) above in such translations, adaptations, summaries, extracts, Derivative Works or Collective Works and (c) to license others to do any or all of the above. The foregoing rights may be exercised in all media and formats, whether now known or hereafter devised, and include the right to make such modifications as are technically necessary to exercise the rights in other media and formats. If the "Open Access" box has been checked in **Item 1** above, JoVE and the Author hereby grant to the public all such rights in the Article as provided in, but subject to all limitations and requirements set forth in, the CRC License.

4. Retention of Rights in Article. Notwithstanding the exclusive license granted to JoVE in **Section 3** above, the Author shall, with respect to the Article, retain the non-exclusive right to use all or part of the Article for the non-commercial purpose of giving lectures, presentations or teaching classes, and to post a copy of the Article on the Institution's website or the Author's personal website, in each case provided that a link to the Article on the JoVE website is provided and notice of JoVE's copyright in the Article is included. All non-copyright intellectual property rights in and to the Article, such as patent rights, shall remain with the Author.

5. Grant of Rights in Video – Standard Access. This **Section 5** applies if the "Standard Access" box has been checked in **Item 1** above or if no box has been checked in **Item 1** above. In consideration of JoVE agreeing to produce, display or otherwise assist with the Video, the Author hereby acknowledges and agrees that, Subject to **Section 7** below, JoVE is and shall be the sole and exclusive owner of all rights of any nature, including, without limitation, all copyrights, in and to the Video. To the extent that, by law, the Author is deemed, now or at any time in the future, to have any rights of any nature in or to the Video, the Author hereby disclaims all such rights and transfers all such rights to JoVE.

6. Grant of Rights in Video – Open Access. This **Section 6** applies only if the "Open Access" box has been checked in **Item 1** above. In consideration of JoVE agreeing to produce, display or otherwise assist with the Video, the Author hereby grants to JoVE, subject to **Section 7** below, the exclusive, royalty-free, perpetual (for the full term of copyright in the Article, including any extensions thereto) license (a) to publish, reproduce, distribute, display and store the Video in all forms, formats and media whether now known or hereafter developed (including without limitation in print, digital and electronic form) throughout the world, (b) to translate the Video into other languages, create adaptations, summaries or extracts of the Video or other Derivative Works or Collective Works based on all or any portion of the Video and exercise all of the rights set forth in (a) above in such translations, adaptations, summaries, extracts, Derivative Works or Collective Works and (c) to license others to do any or all of the above. The foregoing rights may be exercised in all media and formats, whether now known or hereafter devised, and include the right to make such modifications as are technically necessary to exercise the rights in other media and formats. For any Video to which this Section 6 is applicable, JoVE and the Author hereby grant to the public all such rights in the Video as provided in, but subject to all limitations and requirements set forth in, the CRC License.

7. Government Employees. If the Author is a United States government employee and the Article was prepared in the course of his or her duties as a United States government employee, as indicated in **Item 2** above, and any of the licenses or grants granted by the Author hereunder exceed the scope of the 17 U.S.C. 403, then the rights granted hereunder shall be limited to the maximum rights permitted under such statute. In such case, all provisions contained herein that are not in conflict with such statute shall remain in full force and effect, and all provisions contained herein that do so conflict shall be deemed to be amended so as to provide to JoVE the maximum rights permissible within such statute.

8. Likeness, Privacy, Personality. The Author hereby grants JoVE the right to use the Author's name, voice, likeness, picture, photograph, image, biography and performance in any way, commercial or otherwise, in connection with the Materials and the sale, promotion and distribution thereof. The Author hereby waives any and all rights he or she may have, relating to his or her appearance in the Video or otherwise relating to the Materials, under all applicable privacy, likeness, personality or similar laws.

9. Author Warranties. The Author represents and warrants that the Article is original, that it has not been published, that the copyright interest is owned by the Author (or, if more than one author is listed at the beginning of this Agreement, by such authors collectively) and has not been assigned, licensed, or otherwise transferred to any other party. The Author represents and warrants that the author(s) listed at the top of this Agreement are the only authors of the Materials. If more than one author is listed at the top of this Agreement and if any such author has not entered into a separate Article and Video License Agreement with JoVE relating to the Materials, the Author represents and warrants that the Author has been authorized by each of the other such authors to execute this Agreement on his or her behalf and to bind him or her with respect to the terms of this Agreement as if each of them had been a party hereto as an Author. The Author warrants that the use, reproduction, distribution, public or private performance or display, and/or modification of all or any portion of the Materials does not and will not violate, infringe and/or misappropriate the patent, trademark, intellectual property or other rights of any third party. The Author represents and warrants that it has and will continue to comply with all government, institutional and other regulations, including, without limitation all institutional, laboratory, hospital, ethical, human and animal treatment, privacy, and all other rules, regulations, laws, procedures or guidelines, applicable to the Materials, and that all research involving human and animal subjects has been approved by the Author's relevant institutional review board.

10. JoVE Discretion. If the Author requests the assistance of JoVE in producing the Video in the Author's facility, the Author shall ensure that the presence of JoVE employees, agents or independent contractors is in accordance with the relevant regulations of the Author's institution. If more than one author is listed at the beginning of this Agreement, JoVE may, in its sole discretion, elect not take any action with respect to the Article until such time as it has received complete, executed Article and Video License Agreements from each such author. JoVE reserves the right, in its absolute and sole discretion and without giving any reason therefore, to accept or decline any work submitted to JoVE. JoVE and its employees, agents and independent contractors shall have

full, unfettered access to the facilities of the Author or of the Author's institution as necessary to make the Video, whether actually published or not. JoVE has sole discretion as to the method of making and publishing the Materials, including, without limitation, to all decisions regarding editing, lighting, filming, timing of publication, if any, length, quality, content and the like.

11. Indemnification. The Author agrees to indemnify JoVE and/or its successors and assigns from and against any and all claims, costs, and expenses, including attorney's fees, arising out of any breach of any warranty or other representations contained herein. The Author further agrees to indemnify and hold harmless JoVE from and against any and all claims, costs, and expenses, including attorney's fees, resulting from the breach by the Author of any representation or warranty contained herein or from allegations or instances of violation of intellectual property rights, damage to the Author's or the Author's institution's facilities, fraud, libel, defamation, research, equipment, experiments, property damage, personal injury, violations of institutional, laboratory, hospital, ethical, human and animal treatment, privacy or other rules, regulations, laws, procedures or guidelines, liabilities and other losses or damages related in any way to the submission of work to JoVE, making of videos by JoVE, or publication in *JoVE* or elsewhere by JoVE. The Author shall be responsible for, and shall hold JoVE harmless from, damages caused by lack of sterilization, lack of cleanliness or by contamination due to the making of a video by JoVE its employees, agents or independent contractors. All sterilization, cleanliness or decontamination procedures shall be solely the responsibility of the Author and shall be undertaken at the Author's expense. All indemnifications provided herein shall include JoVE's attorney's fees and costs related to said losses or damages. Such indemnification and holding harmless shall include such losses or damages incurred by, or in connection with, acts or omissions of JoVE, its employees, agents or independent contractors.

12. Fees. To cover the cost incurred for publication, JoVE must receive payment before production and publication the Materials. Payment is due in 21 days of invoice. Should the Materials not be published due to an editorial or production decision, these funds will be returned to the Author. Withdrawal by the Author of any submitted Materials after final peer review approval will result in a US$1,200 fee to cover pre-production expenses incurred by JoVE. If payment is not received by the completion of filming, production and publication of the Materials will be suspended until payment is received.

13. Transfer, Governing Law. This Agreement may be assigned by JoVE and shall inure to the benefits of any of JoVE's successors and assignees. This Agreement shall be governed and construed by the internal laws of the Commonwealth of Massachusetts without giving effect to any conflict of law provision thereunder. This Agreement may be executed in counterparts, each of which shall be deemed an original, but all of which together shall be deemed to me one and the same agreement. A signed copy of this Agreement delivered by facsimile, e-mail or other means of electronic transmission shall be deemed to have the same legal effect as delivery of an original signed copy of this Agreement.

A signed copy of this document must be sent with all new submissions. Only one Agreement required per submission.

CORRESPONDING AUTHOR:

Name:	Aji P Mathew
Department:	Materials and Environmental Chemistry
Institution:	Stockholm University, Sweden
Article Title:	3D printed porous cellulose nanocomposite hydrogel scaffolds
Signature:	
Date:	8 January 2019

Please submit a signed and dated copy of this license by one of the following three methods:

1) Upload a scanned copy of the document as a pfd on the JoVE submission site;
2) Fax the document to +1.866.381.2236;
3) Mail the document to JoVE / Attn: JoVE Editorial / 1 Alewife Center #200 / Cambridge, MA 02139

For questions, please email submissions@jove.com or call +1.617.945.9051

Response to comments

Ref: JoVE submission JoVE59401 entitled 3D printed porous cellulose nanocomposite hydrogel scaffolds

We would like to thanks editor and reviewers for their time and feedback.

Editorial comments:

1. Please take this opportunity to thoroughly proofread the manuscript to ensure that there are no spelling or grammar issues.
Thank you for your comment. We have proofread the manuscript.
2. The Summary is over the 50 word limit.
Thank you for your comment. Summary is revised now.
3. There is a 2.75 page limit for filmable content. Please highlight 2.75 pages or less of the Protocol steps in yellow (including headings and spacing) for filming that identifies the essential steps of the protocol for the video, i.e., the steps that should be visualized to tell the most cohesive story of the Protocol.
Please find the highlighted text in the manuscript.
4. JoVE cannot publish manuscripts containing commercial language. This includes company names before an instrument or reagent. Please remove all commercial language from your manuscript and use generic terms instead. All commercial products should be sufficiently referenced in the Table of Materials and Reagents. Examples of commercial language in your manuscript include BioPuls, etc.
Thank you for the explanation. Commercial language is removed now.
5. Please use a single space between numerical values and their units.
Thank you for your comment. The space is corrected now.
6. Please use h, min, s for time units.
Thank you for your comment. The units are revised now.
7. Step 4.5: Please write this step in the imperative tense.
Thank you for your comment. The step wording is revised now.
8. Please number all references in Reference section.
Thank you for your comment. The references are numbered now.
9. Please sign the Author license agreement and check the Standard Access form.
Thank you for your comment. Standard access is checked now.